JMEPEG (2008) 17:607–611
DOI: 10.1007/s11665-007-9189-x

1059-9495/$19.00

Tensile Deformation of a Nickel-base Alloy at Elevated Temperatures

Ajit K. Roy, Anand Venkatesh, Vikram Marthandam, and Arindam Ghosh

(Submitted June 8, 2007; in revised form November 28, 2007)

The results of tensile testing involving Waspaloy indicate that the failure strain was gradually reduced at temperatures ranging between ambient and 300 °C. Further, serrations were observed in the engineering stress versus strain diagrams in the temperature range of 300-600 °C. The reduced failure strain and the formation of serrations in these temperature regimes could be the result of dynamic strain aging of this alloy. The extent of work hardening due to plastic deformation was reduced at temperatures above 300 °C. A combination of ductile and intergranular brittle failures was seen at temperatures above 600 °C. γ′ was detected at all tested temperatures.

Keywords fractography, tensile deformation, Waspaloy, work-hardening index

1. Introduction

Generation of hydrogen using a thermochemical process, known as sulfur-iodine (S-I) cycle, has been considered in recent years (Ref 1-3). Heat from nuclear reactors will be used to accommodate chemical reactions involving the formation and decomposition of sulfuric acid (H_2SO_4) and hydrogen iodide (HI), leading to the generation of oxygen (O_2) and hydrogen (H_2), respectively. A maximum temperature of 950 °C has been recommended to achieve the highest possible efficiency in hydrogen generation using the S-I process, which is illustrated in Fig. 1. It is obvious that the primary challenge in developing H_2 using nuclear heat and chemical reactions is the identification and selection of suitable structural materials possessing superior tensile properties at elevated temperatures and an excellent corrosion resistance in the presence of aggressive chemical species.

Austenitic nickel (Ni)-base Waspaloy (UNS N07001) has been investigated in this study to evaluate its tensile properties at temperatures relevant to the S-I process. The identification of Waspaloy as a candidate structural material in nuclear hydrogen generation was based on its excellent high temperature tensile properties and superior corrosion resistance in many hostile environments (Ref 4-6). This article presents the results of tensile testing of Waspaloy at temperatures ranging from ambient to 1000 °C, elucidating a plausible mechanism of its deformation in terms of work-hardening index (n) and fracture morphology.

Ajit K. Roy, Anand Venkatesh, Vikram Marthandam, and **Arindam Ghosh**, Department of Mechanical Engineering, University of Nevada Las Vegas (UNLV), 4505 Maryland Parkway, Box 454027, Las Vegas, NV 89154-1027. Contact e-mail: aroy@unlv.nevada.edu.

2. Experimental Procedures

Round bars of Waspaloy were procured from a vendor in a heat-treated condition, which consisted of annealing at 1052 °C (1925 °F) followed by water quenching. The chemical composition of this alloy is shown in Table 1. Large austenitic grains and annealing twins were seen in the optical micrograph of the as-received material, as shown in Fig. 2. No additional thermal treatments were given to Waspaloy prior to the fabrication of the smooth cylindrical specimens for tensile properties evaluation. The specimens were machined in such a way that the gage section was parallel to the rolling direction. A ratio of 4 was maintained between the gage length and the gage diameter of these specimens to comply with the ASTM designation E 08 2004 (Ref 7). These specimens had an overall length of 101.6 mm (4 in.), a gage length of 25.4 mm (1 in.), and a gage diameter of 6.35 mm (0.25 in.).

The tensile properties of Waspaloy including yield strength (YS), ultimate tensile strength (UTS), percent elongation (%El), and percent reduction in area (%RA) were determined using a commercially available testing equipment at temperatures ranging from ambient to 1000 °C. A custom-made, ceramic-lined split furnace was attached to this equipment for determination of the tensile properties at elevated temperatures. Nitrogen was continuously spurged during testing at elevated temperatures to prevent contamination/oxidation of the specimen surface. The specimens were strained at a rate of 10^{-3} s^{-1} under tensile loading. The engineering stress versus engineering strain (s-e) diagrams were automatically generated using this equipment.

The extent of work hardening due to plastic deformation of engineering metals and alloys is known to be related to both the true stress (σ) and the true strain (ε) according to the Hollomon equation (Eq 1) (Ref 8-11). K in this equation is a constant, known as the strength coefficient. The magnitude of work-hardening index, indicated by n, can be determined from the slope of a straight line obtained by plotting log σ versus log ε for a specimen tested in tension at a specific temperature. However, since a linear relationship could not be obtained in this investigation, the magnitude of n was determined by

modifying Eq 1 through inclusion of a second term (Δ). Δ can be given by [exp($K_1 + n^1$ ε)], where K_1 and n^1 represent an intercept and the slope of the line, respectively, generated from the plot of log Δ versus log ε. Such modification in the σ versus ε relationship, as shown by Eq 2, is known as the Ludwigson equation (Ref 10-12).

$$\sigma = K\varepsilon^n \quad \text{(Eq 1)}$$

$$\sigma = (K\varepsilon^n + \Delta) \quad \text{(Eq 2)}$$

In view of the resultant non-linear relationship, the magnitude of *n* was determined using the best linear portion of the log σ versus log ε plot, where Δ was assumed to have a value of zero. The value of *n* was computed from the slope of this line, as shown in Fig. 3 for a specimen tested at ambient temperature. The values of *n* at other temperatures were determined using a similar approach.

The extent and morphology of failure at the primary fracture surface of all tested specimens were determined by scanning electron microscopy (SEM). Energy dispersive spectroscopy (EDS) was used for elemental analysis in the vicinity of these failures. Further, X-ray diffractometry (XRD) was used to determine the presence or absence of precipitates/secondary phases, if any.

3. Results and Discussion

The results of tensile testing of Waspaloy are illustrated in Fig. 4 in the form of a superimposed s-e diagram as a function of the testing temperature. As anticipated, the magnitudes of YS, UTS, and failure stress were gradually reduced with increasing temperature. It is interesting to note that no distinction could be made between YS and UTS at temperatures above 800 °C, indicating an absence of uniform strain at significantly higher temperatures. The variations of all four tensile parameters (YS, UTS, %El, and %RA) derived from the s-e diagrams and the specimen dimensions, before and after replicate testing, are given in Table 2.

An evaluation of the tensile data clearly indicates that the failure strain in terms of %El was gradually reduced within a temperature range of ambient to 300 °C. The reduced ductility in terms of %El with increasing temperature, as seen here, has often been cited (Ref 8) to be the result of dynamic strain aging (DSA) associated with the work-hardening of a susceptible

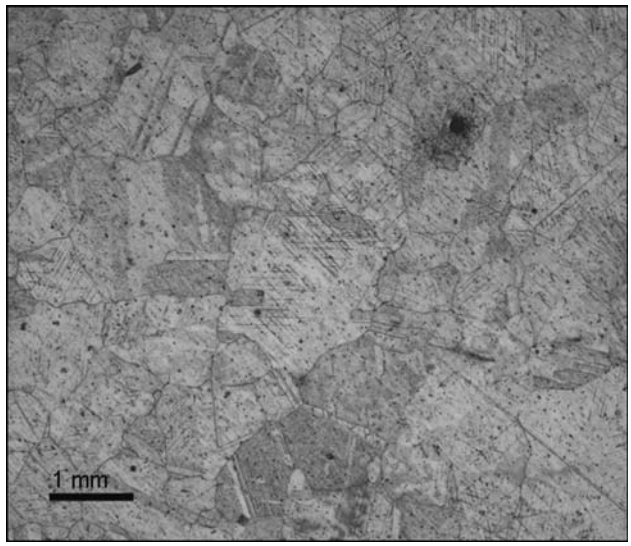

Fig. 2 Optical micrograph, 1 mL HCl + 10 mL acetic acid + 5 mL HNO_3, 100×

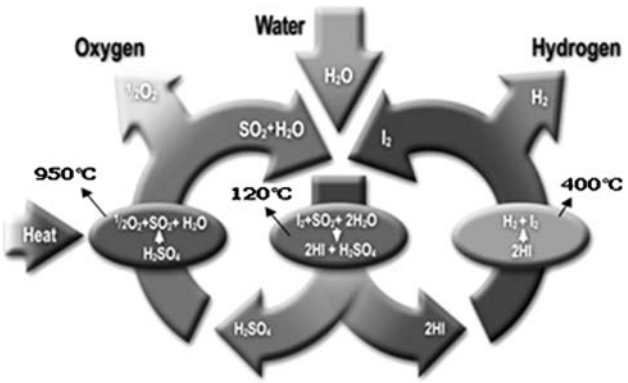

Fig. 1 S-I cycle

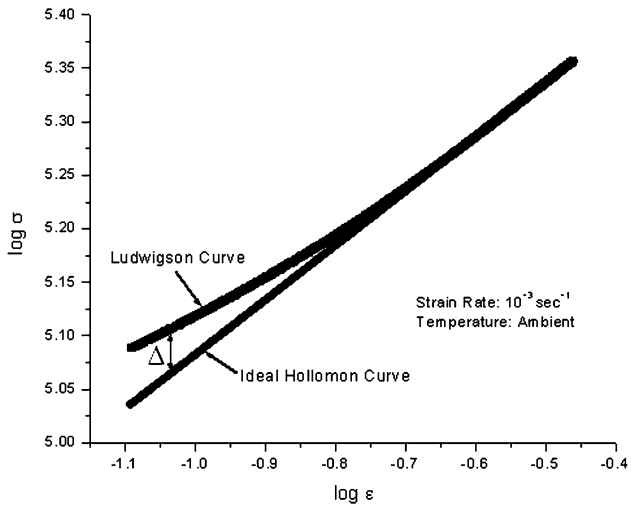

Fig. 3 log σ versus log ε for *n* calculation

Table 1 Chemical composition of Waspaloy

	Elements, wt.%													
Heat no.	**C**	**Co**	**Cr**	**Fe**	**Mn**	**Mo**	**Ni**	**P**	**Al**	**Ti**	**Ta**	**Si**	**V**	**W**
GH55	0.044	13.11	19.40	0.08	0.01	4.23	58.61	0.002	1.39	3.03	0.02	0.02	0.01	0.02

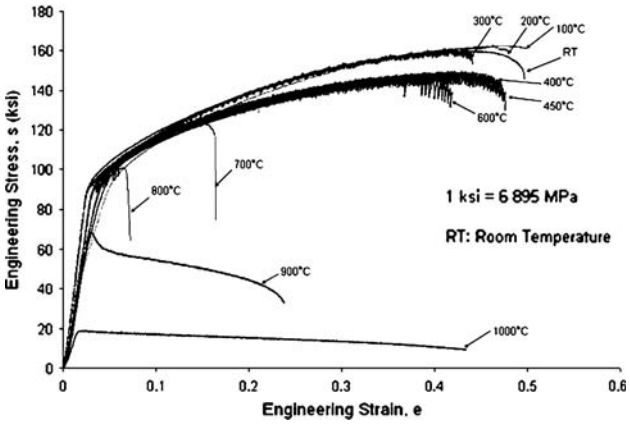

Fig. 4 s-e diagram versus temperature

Table 2 Tensile properties versus temperature

Temperature, °C	YS, ksi/MPa	UTS, ksi/MPa	%El	%RA
Ambient	99/684	178/1226	50.6	45.0
100	95/657	165/1138	48.1	47.0
200	93/641	163/1123	47.9	48.1
300	89/615	161/1111	44.1	48.7
400	87/600	150/1035	47.3	49.8
450	87/599	149/1030	47.9	50.0
600	86/595	146/1007	41.9	50.9
700	85/586	115/793	17.4	31.0
800	83/570	93/641	7.1	15.3
900	68/469	69/476	24.0	38.0
1000	18/125	19/131	41.0	43.2

material due to tensile loading at relatively lower temperatures. A similar phenomenon has been reported for other nickel-base austenitic materials including Alloy C-276 (Ref 13). The occurrence of DSA is known to be the result of solute diffusion within a susceptible temperature regime (Ref 14-17), thus, impeding the movement of dislocations generated during plastic deformation. At relatively higher temperatures (400 and 450 °C), the ductility in terms of %El was enhanced, possibly due to a greater dislocation mobility. Interestingly, serrations of varied heights were also seen in the s-e diagrams at temperatures ranging from 300 to 600 °C that are also known to be associated with the occurrence of DSA (Ref 13).

The average n values, determined for specimens tested at room temperature, 100, 200, 300, 400, and 450 °C using Hollomon and Ludwigson relationships, are given in Table 3. An evaluation of these data indicates that between ambient temperature and 300 °C, the magnitude of n ranged between 0.48 and 0.52, showing an insignificant variation of this parameter. However, the magnitude of n was reduced to some extent at temperatures above 300 °C, suggesting that the ductility was enhanced at elevated temperatures due to the ease of plastic flow. This observation is consistent with the higher

Table 3 *n* versus temperature

Temperature, °C	*n*
Ambient	0.48
100	0.51
200	0.52
300	0.48
400	0.43
450	0.40

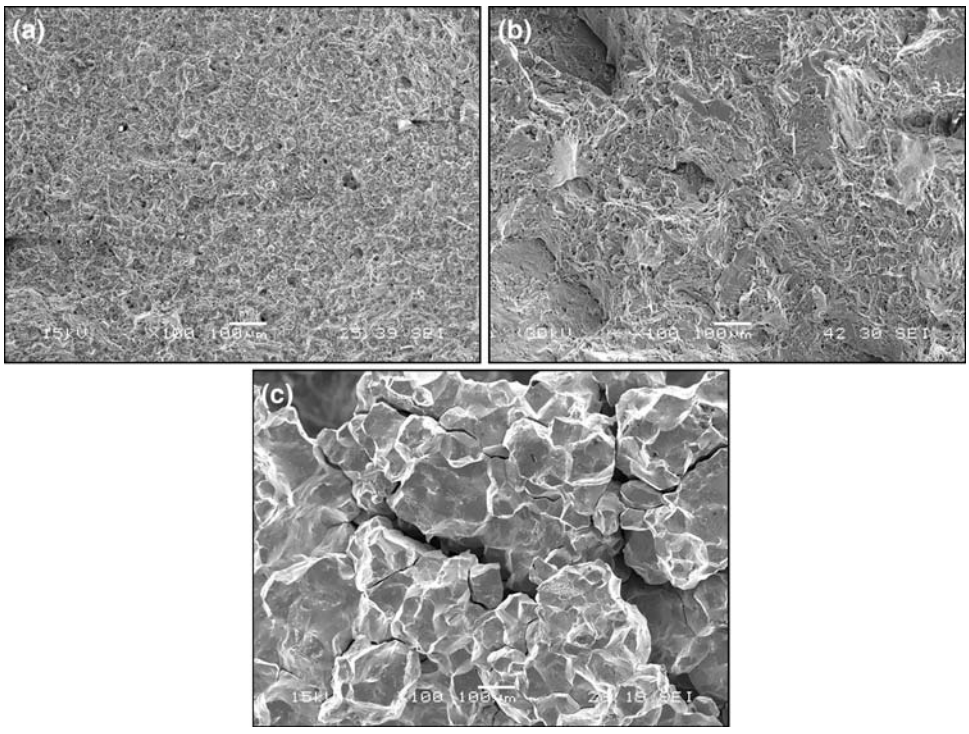

Fig. 5 SEM micrographs of tested tensile specimens: (a) ambient temperature, (b) 600 °C, and (c) 800 °C

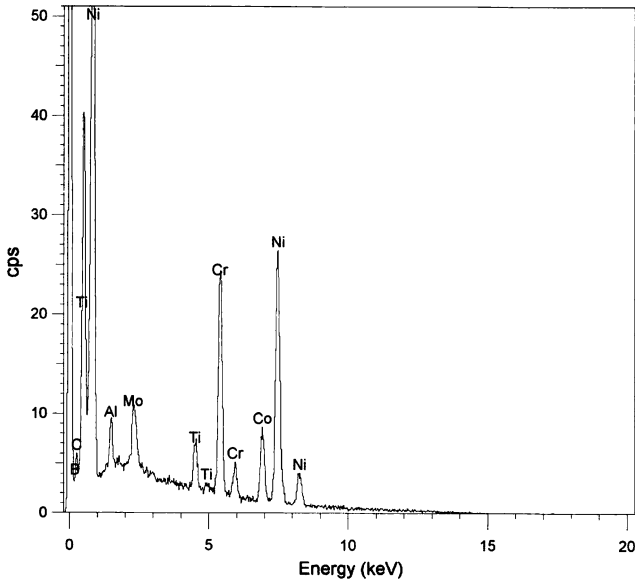

Fig. 6 EDS spectrum for specimen tested at 800 °C

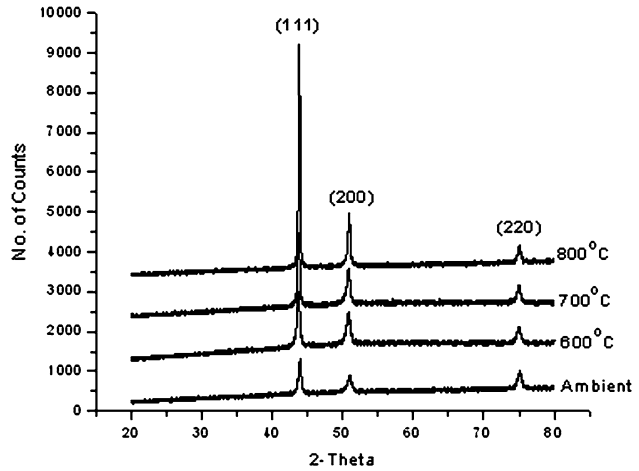

Fig. 7 XRD profile versus temperature

ductility in terms of the calculated %El at 400 and 450 °C, as shown in Table 2. No technical data currently exist in the open literature on the variation of n with temperature for an austenitic alloy such as Waspaloy. Thus, a comparison of the resultant n values to the literature data cannot be made.

The evaluation of the primary fracture surface of the specimens tested at temperatures ranging between ambient and 600 °C by SEM revealed dimpled microstructures, indicating predominantly ductile failures. However, a combination of ductile and intergranular brittle failures was seen in the SEM micrographs of the specimens tested at temperatures above 600 °C, as shown in Fig. 5. EDS was performed in the vicinity of cracks to identify deleterious species, if any. However, the EDS spectrum, shown in Fig. 6, exhibited only the major elements present in Waspaloy. Subsequently, XRD was used to determine the presence or absence of precipitates/secondary phases that could possibly be responsible for brittle failure of Waspaloy at temperatures above 600 °C. The indexed peaks, determined from the XRD analyses (Fig. 7), matched the fundamental FCC reflections of the gamma prime (γ') phase, known (Ref 18) to be present in Waspaloy.

4. Summary and Conclusions

The tensile properties of Waspaloy have been evaluated at temperatures ranging from ambient to 1000 °C. SEM, EDS, and XRD have been employed to develop a basic understanding of tensile deformation of this alloy as a function of the testing temperature. The key results and the significant conclusions derived from this investigation are summarized below:

- The tensile strength of Waspaloy in terms of YS and UTS was gradually reduced with increasing temperature. Beyond 800 °C, no uniform strain was seen in the s-e diagrams.
- The failure strain (e_f) was gradually reduced within a temperature range of ambient to 300 °C, followed by an irregular variation at higher temperatures. Serrations of different heights were also noted in the s-e diagrams for specimens tested at temperatures ranging from 300 to 600 °C.
- Reduced e_f and the occurrence of serrations within specific temperature regimes may be attributed to the phenomenon of DSA.
- The magnitude of n was reduced at temperatures above 300 °C due to the ease of plastic deformation at higher temperatures.
- Dimpled microstructures, indicating ductile failures, were seen in the SEM micrographs of specimens tested at temperatures up to 600 °C. However, a combination of ductile and intergranular brittle failures was seen in the specimens tested at higher temperatures.
- The XRD technique was capable of identifying the γ' phase in specimens tested both at ambient and elevated temperatures.

Acknowledgment

The financial support of the United States Department of Energy under grant number DE-FC07-04ID14566 is thankfully acknowledged.

References

1. A.K. Roy and A.V. Kaiparambil, Tensile and Corrosion Behavior of Zr705 for Nuclear Hydrogen Generation, *Mater. Sci. Eng. A*, 2006, **427**(1–2), p 320–326
2. A.K. Roy and V. Virupaksha, Performance of Alloy 800H for High-Temperature Heat Exchanger Applications, *Mater. Sci. Eng. A*, 2007, **452–453**, p 665–672
3. D. O'Keefe, C. Allen, G. Besenbruch, L. Brown, J. Norman, and R. Sharp, Preliminary Results from Bench-Scale Testing of a Sulfur–Iodine Thermochemical Water-Splitting Cycle, *Int. J. Hydrogen Energy*, 1982, **7**(5), p 381–392
4. X. Wei, Experimental Study on the Machining of a Shaped Hole in Ni-Based Super-Heat-Resistant Alloy, *J. Mater. Process. Technol.*, 2002, **129**, p 143–147

5. J.K. Yelavarthi, High-Temperature Deformation and Environment-Induced Degradation of Waspaloy, M.S. Thesis, University of Nevada Las Vegas, 2006
6. L. Savalia, Performance of Waspaloy at Elevated Temperature for Heat Exchanger Applications, M.S. Thesis, University of Nevada Las Vegas, 2006
7. Standard Test Methods for Tension Testing of Metallic Materials, E 8-4, *Annual Book of ASTM Standards*, ASTM International, 2004, p 86–109
8. R. Kishore, R.N Singh, T.K Sinha, and B.P. Kashyap, Effect of Dynamic Strain Aging on the Tensile Properties of a Modified 9Cr-1Mo steel, *J. Mater. Sci.*, 1997, **32**(199), p 437–442
9. V. Raghavan, Mechanical Properties, *Physical Metallurgy Principles and Practice*, 1996, Prentice-Hall of India, p 141–146
10. K.G. Samuel, Limitations of Hollomon and Ludwigson Stress-Strain Relations in Assessing the Strain Hardening Parameters, *J. Phys. D Appl. Phys.*, 2006, **39**, p 203–212
11. H. Hollomon, *Trans. AIME*, 1945, **162**, p 268–269
12. D.C. Ludwigson, Modified Stress-Strain Relation for FCC Metals and Alloys, *Metall. Mater. Trans. A*, 1971, **2**, p 2825–2828
13. A.K. Roy. J. Pal, and C. Mukhopadhyay, Dynamic Strain Ageing of an Austenitic Superalloy-Temperature and Strain Rate Effects, *Mater. Sci. Eng. A*., in press
14. V. Shankar, M. Valsan, K.B.S. Rao, and S.L. Mannan, Effects of Temperature and Strain Rate on Tensile Properties and Activation Energy for Dynamic Strain Aging in Alloy 625, *Metall. Mater. Trans. A*, 2004, **35**, p 3129–3139
15. S.H. Hong, H.Y. Kim, J.S. Jang, and I.H. Kuk, Dynamic Strain Aging Behavior of Inconel 600 Alloy, *Superalloys*, Sept 22–26, 1996 (Champion, Pennsylvania), The Minerals, Metals and Materials Society, p 401–408
16. A. Girones, L. Llanes, M. Anglada, and A. Mateo, Dynamic Strain Aging Effects on Super Duplex Stainless Steels at Intermediate Temperatures, *Mater. Sci. Eng. A.*, 2004, **367**(1–2), p 322–328
17. L.H. Almeida and P.R.O. Emygdio, Activation Energy Calculation and Dynamic Strain Ageing in Austenitic Stainless Steel, *Scripta Metall. et Mater.*, 1994, **31**, p 505–510
18. V. Siva Kumar, G. Kelekanjeri, and R.A. Gerhardt, Characterization of Microstructural Fluctuations in Waspaloy Exposed to 760 °C for Times up to 2500 h, *Electrochim. Acta*, 2006, **51**, p 1873–1880